sciendo

DOI: 10.2478/awutp-2019-0005

ANNALS OF WEST UNIVERSITY OF TIMISOARA PHYSICS
Vol. LXI, 2019

SPIN COATING METHOD FABRICATED OF In_2O_3 THIN FILMS

Said Benramache [1,*], Yacine Aoun [2]

[1] *Material Sciences Department, Faculty of Science, University of Biskra 07000, Algeria*

[2] *Department of Mechanics, University of El-oued, Algeria*

**Corresponding author: Email: s.benramache@univ-biskra.dz*

Article Info	Abstract
Received: 17.12.2019 *Accepted: 06.01.2020* **Keywords:** In_2O_3, Thin films, Spain coater method, Crystalline structure, Transmission	In this work, the In_2O_3 thin films have been fabricated using a spin coating technique; this technique was prepared in our laboratory. The effect of the layer times (3, 5, 7 and 9 times) on optical and structural properties was investigated. In_2O_3 thin films were fabricated by dissolving 0.2 M of the indium chloride dehydrate $InCl_3.2H_2O$ in the absolute H2O. The In_2O_3 thin films were crystallized at a temperature of 600 °C with pending time of 1 hour. The optical property shows that the prepared In_2O_3 thin films for 3 and 5 times have a transmission of about 85 %. The maximum bandgap energy was 3.69 eV for 5 times and the lowest Urbach energy was 0.47 eV for 9 times. From XDR all fabricated In_2O_3 thin films having one diffraction crystal plan is (222) peak intensity, this attribution have good crystalline structure with minimum crystallite size of the (222) plan is 59.69 nm. The prepared In_2O_3 thin films can be used in photovoltaic applications due to the existing phase and higher transmission.

1. Introduction

In previous researches, in the field of materials science, several excellent classes have investigated that lead to the synthesis and characterization of thin films as metal oxides (semiconductors) [1]. In_2O_3 has one of the most important applications in the detection of bacteria in nature, the presence of bacteria in the environment due to the increase in peoples and industries. So it becomes important to investigate In_2O_3 as a thin film and improve its physical properties. These materials can be developed as photovoltaic applications due to show high transmission overcoming 90% [2], which was located in the visible region. However, the In_2O_3 thin films can be used in several fields in sciences and technology due to their physical and chemical properties such as highly transparent, good crystalline structure, best electrical conductivity and the ease of chemical mixing in any solution [3]. As well as the In_2O_3 thin films are requirements of the general environment to protect it can be focused

on it is a class of good vector of the semiconductor materials due to the n-types in nature [4]. The optical band gap of In_2O_3 thin films was located in the range of 3.5 - 4 eV, which is varied by various conditions like deposition method, precursor molarity, substrate temperature, film thickness, crystallization temperature and doping level [1-5].

In_2O_3 thin films can be fabricated by several techniques such as electrochemical deposition, pulsed laser deposition (PLD), magnetron sputtering technique, molecular beam epitaxy (MBE), reactive evaporation, sol-gel process, chemical vapor deposition, and spray pyrolysis [1–5].

The aim of this work is to fabricate In_2O_3 thin films with good transmission and good crystalline structure. The films were fabricated with 0.2 M at a crystallization temperature of 600 °C. We have studied the influence of several layer times on optical transmission, bandgap energy, Urbach energy, crystalline structure and crystallite size of In_2O_3 thin films.

2. Experiments

The prepared solution of In_2O_3 was investigated by dissolving the 0.2 M of the indium chloride dehydrates $InCl_3.2H_2O$ in the absolute H_2O, HCl was used as stabilization of In_2O_3 solution. This solution has been stirred a heated at 50 °C for one hour to have a solution with high transparent. The film coating was deposited two days after the preparation.

The In_2O_3 thin films were deposited by dropping the In_2O_3 solution on the microscopic glass substrate, which are prepared at room temperature by a spin coating method. The experimental conditions were applied to obtain a good quality of In_2O_3 thin films, which was rotated between 2000 to 2500 rpm for the 20s. The In_2O_3 thin films have been deposited at different coating times are 3, 5, 7 and 9 times. The In_2O_3 thin films were pre-heated at a temperature of 100 °C, and then crystallized at 600 °C with a pending time of 1 hour.

The In_2O_3 thin films were characterized to obtain the optical transmission, bandgap energy, Urbach energy, crystalline structure and crystallite size of In_2O_3 thin films. The optical transmission of the In_2O_3 thin films was obtained using by an ultraviolet-visible spectrophotometer (LAMBDA 25) in the range of 300–1000 nm. However, the crystalline structure was carried by X-ray diffraction (XRD Bruker AXS-8D, CuKα, $\lambda = 0.15406$ nm) in the scanning range of ($2\theta = 30°$ to 40°).

3. Results and discussion

The optical transmission of deposited In_2O_3 thin films is shown in Fig. 1, presents with various coating times of deposited films. As seen, the optical transmission of deposited In_2O_3

thin films was decreased with increasing coating times, we have observed a higher transmission of about 85% in the visible region. However, in the ultraviolet region the optical transmission decreased because of the absorption edge. Fig. 2 shows the absorbance of deposited In_2O_3 thin films at various coating times, we have concluded that the thin film prepared with 9 coating times has the maximum absorption.

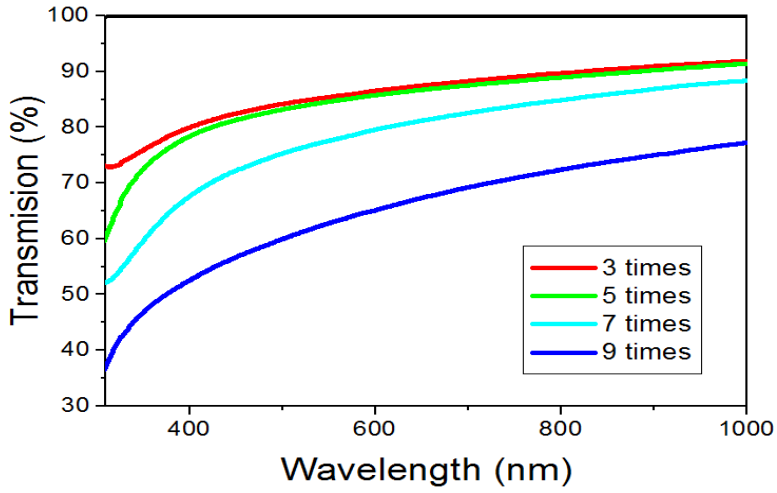

Fig.1. Variation of transmission spectra (T) with wavelength (λ) of deposited In_2O_3 thin films at different coating times.

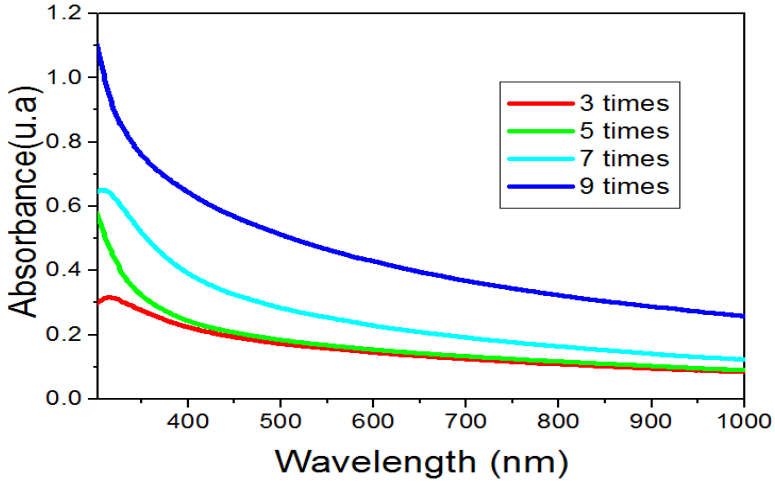

Fig.2. Variation of absorbance spectra (A) with wavelength (λ) of deposited In_2O_3 thin films at different coating times.

The optical bandgap energy of deposited In_2O_3 thin films were estimated from visible region, it was determined by following equation [6]:

$$(Ah\upsilon)^2 = B(h\upsilon - E_g) \quad (1)$$

where A, $h\nu$ C and E_g are the absorbance, the photon energy, a constant and the bandgap

energy of deposited In_2O_3 thin films, respectively. The variation bandgap was calculated using the Fig. 3, which is determined by the extrapolation. However, the tail width can be calculated using the Urbach energy of deposited In_2O_3 thin films also was determined by the following equation [6]:

$$A = A_0 \exp\left(\frac{h\upsilon}{E_u}\right) \tag{2}$$

where A, $h\nu$, A_0 and E_u are the absorbance, the photon energy, a constant and the Urbach energy, respectively. The Urbach energy of fabricated In_2O_3 thin films was determined by deducing the curves of LnA with the variation of the photon energy $h\nu$ (see Fig. 4) to obtain of the variation Urbach energy of In_2O_3 thin films.

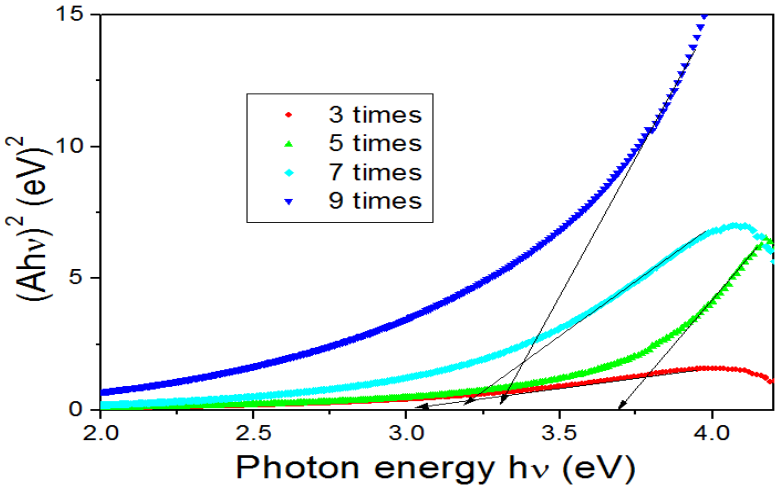

Fig.3. The graph of $(Ah\nu)^2$ versus $h\nu$ plots of In_2O_3 thin films for the bandgap energy.

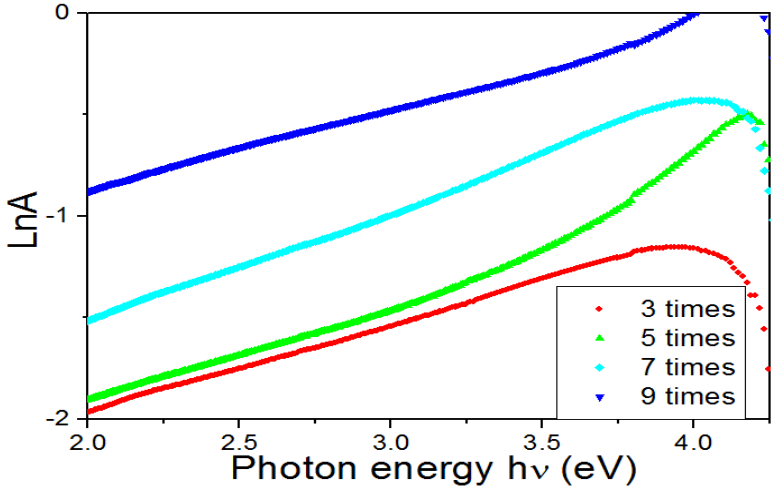

Fig.4. The graph of LnA versus $h\nu$ plots of prepared In_2O_3 thin films for Urbach energy E_u.

Table 1. Optical characterization of In_2O_3 thin films at several layer times.

Layer times	E_g[a] (eV)	E_u[b] (meV)
3	3.03	0.62
5	3.69	0.53
7	3.18	0.58
9	3.30	0.47

[a.] Optical bandgap energy
[b.] Urbach energy

Reported in Fig. 5 and Table 1 with the variation of the layers times' the bandgap energy E_g and the Urbach energy E_u of fabricated In_2O_3 thin films, we have seen that the change in the optical bandgap energy is opposite to the change in the Urbach energy. As can be seen, the optical bandgap energy of prepared In_2O_3 thin a film has the high value was obtained for the thin film fabricated with 5 times, it is 3.69 eV. After this point it is has a minimum value was 3.18 eV for 7 times. However, the Urbach energy has the lowest value was 0.53 eV for 5 times and the highest at 7 times is 0.58 eV. The decrease of bandgap energy with increasing layer times caused by the oxygen diffusion with the deposition. However, the increase of the Urbach energy of prepared In_2O_3 thin films can be explained by increasing of the defects in the films with increasing film thickness.

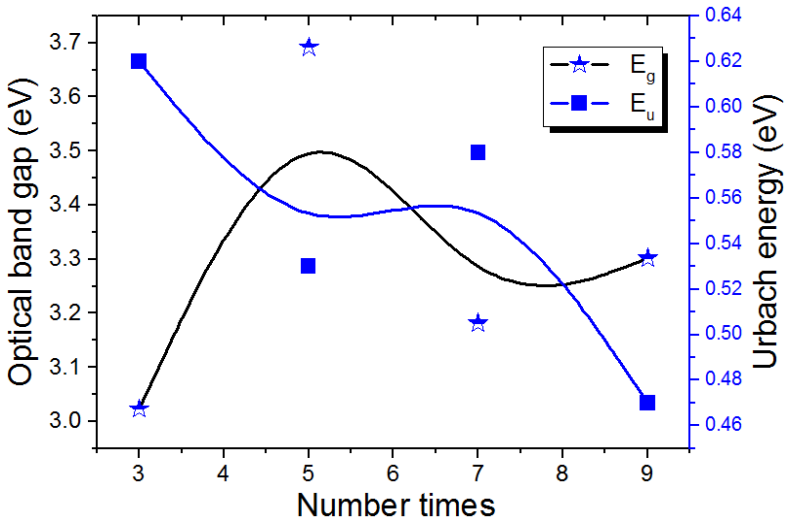

Fig.5. Variation as a function of the layer times of the bandgap energy and Urbach energy of in In_2O_3 thin films.

The X-ray diffraction was used in this work to determine the crystalline structure of In_2O_3 thin films, the results are shown in Fig. 6. The XRD was investigated in the range of

2θ = 30° to 40°. As seen, some In_2O_3 thin films detected three diffraction peaks, are (222), (400) and (411) peaks. With the increase of layer times, we have improved in the peak intensity of the (222) peak, this shows that the elaborated In_2O_3 thin films have a crystalline structure with a preferred orientation to the (222) plan. However, Fig. 6 presents the measured diffraction angle of the (222) peak at several layer times. As seen, the diffraction angle of the (222) peak increased caused by the shifted of (222) peal to the high angle, this attribution can be explained by the decrease in the lattice parameters of the structure of In_2O_3 thin films with the increase in the layer times of deposition.

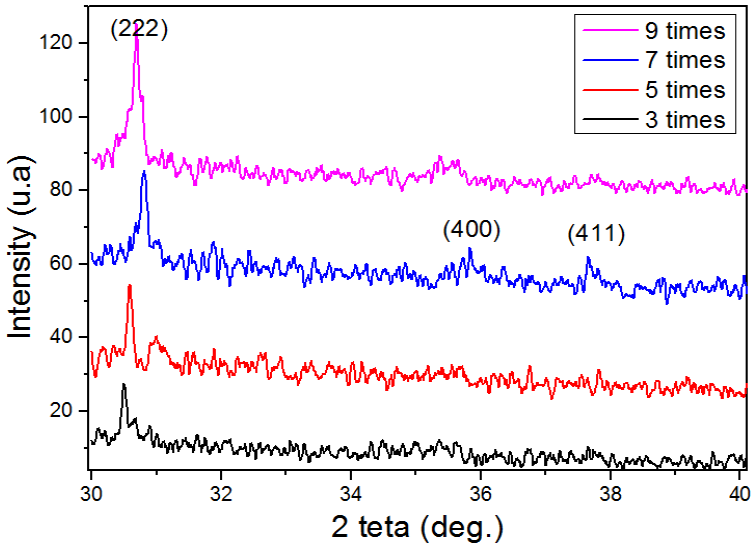

Fig.6. The X-ray diffraction of the crystalline structure of In_2O_3 thin films at several layer times.

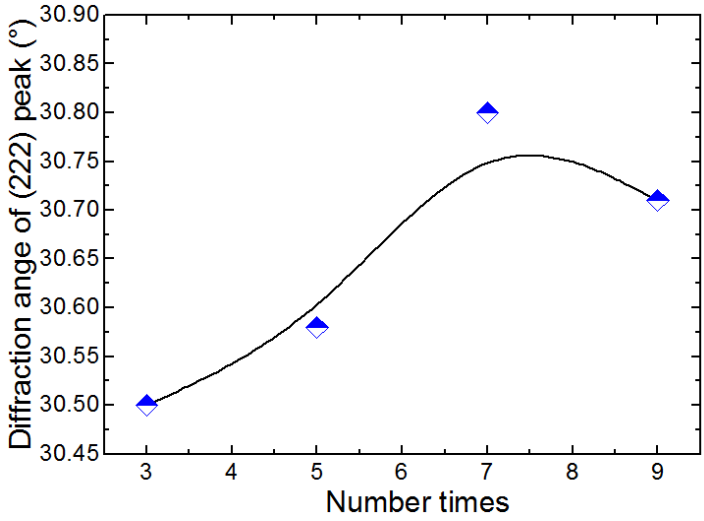

Fig.7. Variation of diffraction angle of the (222) peak of In2O3 thin films at several layer times.

The crystallite G of (222) crystal plane of fabricated In_2O_3 thin films at several layer times was measured by the Scherer equation [8]:

$$G = \frac{0.9\lambda}{\beta \cos\theta} \tag{3}$$

where G is the measured crystallite size at several layer times, λ is the X-ray wavelength (λ = 0.15406 nm), β is the FWHM (full width at half-maximum, and θ is the diffraction angle of the (222) plane crystal plane, the variations are shown in Table 2. Fig. 8 shows the measured crystallite size at several layer times 3, 5, 7 and 9 times of the fabricated In_2O_3 thin films by a spin coating method. We have a decrease of measured crystallite size with increasing layer times from 3 to 9 times, the intensity of (222) peak also increased when the layer times increased, this observation has been indicated to improve the crystallinity and the preferred orientation of prepared In_2O_3 thin films.

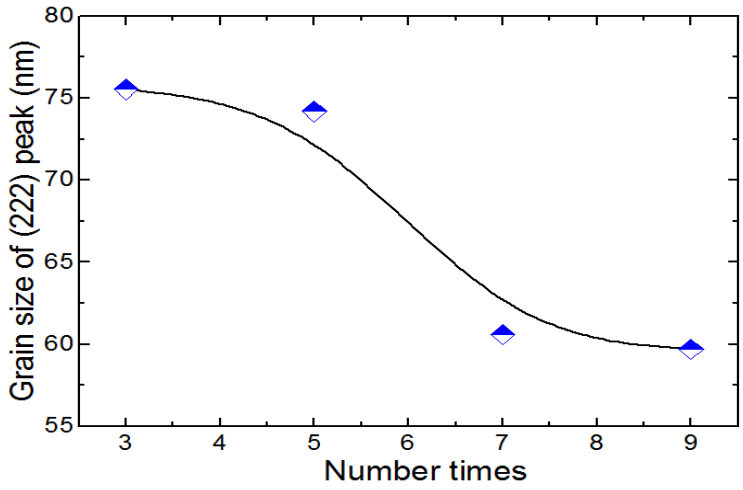

Fig.8. Variation of measured crystallite size of In2O3 thin films at several layer times.

Table 2. Structural characterization of In_2O_3 thin films at several layer times.

Layer times	G[a] (nm)	θ[b] (°)
3	75.54	30.50
5	74.19	30.58
7	60.58	30.80
9	59.69	30.71

[a.] Measured crystallite size

[b.] Diffraction angle of the (222) peak

4. Conclusions

In this work, we have investigated the effect of layers times on the optical and structural characterization of the fabricated In_2O_3 thin films by spin coating technique. In_2O_3 thin films were fabricated by dissolving the indium chloride dehydrate $InCl_3.2H_2O$ in the absolute H_2O, the solution was deposited on a glass substrate by varying the layer times 3, 5, 7 and 9 times, the thin films were crystallized at 600°C. The obtained In_2O_3 thin films have a good optical transmission of about 85% for the smeller layer times. The maximum bandgap energy was 3.69 eV for 5 times and the lowest Urbach energy was 0.47 eV for 9 times. From XDR all fabricated In_2O_3 thin films having one diffraction crystal plan is (222) peak intensity, this attribution have good crystalline structure with minimum crystallite size of the (222) plan is 59.69 nm. The prepared In_2O_3 thin films can be used in photovoltaic applications due to the existing phase and higher transmission.

Acknowledgments

X-ray diffraction data in this work were acquired with an instrument supported by the University of Biskra. We thank Mr. B. Gasmi (Biskra University) for the assistance in XRD data acquisition.

References

[1] K. Sajilal, A. Moses Ezhil Raj, Optik 127 (2016) 1442–1449.

[2] J. Robertson, S.J. Clark, Physical Review B 83 (2011) 075205.

[3] M.V. Frischbier, H.F. Wardenga, M. Weidner, O. Bierwagen, J. Jia, Y. Shigesato, A. Klein, Thin Solid Films 614 (2016) 614, 62–68.

[4] M. Weidner, A. Fuchs, T.J.M. Bayer, K. Rachut, P. Schnell, G.K. Deyu, A. Klein, Advanced Functional Materials 29 (2019) 1807906.

[5] M.A. Fakhri, Engineering and Technology Journal 32 Part (A) (2014) 1323-1330.

[6] W.J. Kim, D. Pradhan, Y. Sohn, Journal of Materials Chemistry A 1 (2013) 10193–10202.

[7] Q. Xiao, H. Zhu, D. Tu, E. Ma, X. Chen, Journal of Physical Chemistry C 117(20) (2013) 10834.

[8] S. Manna, R. Aluguri, R. Bar, S. Das, N. Prtljaga, L. Pavesi, S.K. Ray, Nanotechnology 26 (2015) 45202.